Desalination and Water Treatment
www.deswater.com
doi: 10.5004/dwt.2023.29155

282 (2023) 1–9
January

Performance of polymeric nanofiltration membranes for non-aqueous systems: experimental results and modeling

Hong Shi*, Limeng Li, Jiahui Lu, Shengyuan Xu, Xiaoyang Hu, Rongxian Zhang, Guoxing Zhu, Weihua Zhu

School of Chemistry and Chemical Engineering, Jiangsu University, Zhenjiang 212013, China, Tel.: +86-0511-88780193; emails: hshi@ujs.edu.cn (H. Shi), 390367858@qq.com (L.M. Li), jasmine_luuu@163.com (J.H. Lu), tyxsy49653127@163.com (S.Y. Xu), 2537978010@qq.com (X.Y. Hu), rong@ujs.edu.cn (R.X. Zhang), zhuguoxing@ujs.edu.cn (G.X. Zhu), sayman@ujs.edu.cn (W.H. Zhu)

Received 10 August 2022; Accepted 28 November 2022

ABSTRACT

Study of membrane performance and permeation model is of great significance for the development of solvent-resistant nanofiltration membranes. In this work, filtration experiments were carried out for ten solutes in methanol and ethanol solvents with two polymeric nanofiltration membranes. The effects of solvent, solute and membrane on the separation performance were investigated. The Donnan-steric-pore nanofiltration transport model (DSPM) based on aqueous nanofiltration was modified for the non-aqueous nanofiltration. It was found that the separation performance of the membrane was dominated by membrane structure parameters, physical properties of solvent and features of solute. The modeling results revealed that the solvent had influences on the average pore radius of the membrane; solute charge, solute-solvent-membrane interactions existed in non-aqueous nanofiltration; and the modified model was suitable to predict rejections of neutral solutes rather than charged solutes in the non-aqueous system. These findings provide a novel modification strategy that could be utilized as a convenient and powerful tool for predicting membrane performance and understanding the separation disciplines of non-aqueous nanofiltration.

Keywords: Nanofiltration; Non-aqueous; Modeling; Organic solvent nanofiltration

1. Introduction

As an alternative for traditional separations such as distillation and evaporation, membrane separation is competitive in saving energy and protecting environments. Transport mechanisms of nanofiltration membrane are not yet clearly understood, especially in non-aqueous systems [1,2]. There are a number of factors involved in it, for example, interactions between the solute/solvent/membrane material; size, charge, and shape of the molecule; swelling effect; etc. [3,4]. The performance of polymeric membrane in the presence of organic solvent appears to be much less predictable than in aqueous solutions, and the molar mass cut-off (MMCO) is an insufficient parameter to characterize the separation ability of the membranes in organic solvents [5]. Permeation models in organic solvent nanofiltration are more complicated than in aqueous media [6–11], which are drawbacks for further implementation.

The transport through membranes has been described by three kinds of models. The first group is based on irreversible thermodynamics and considers the membrane as a black box, without accounting for any membrane property. The models are the Kedem–Katchalsky and the

* Corresponding author.

Spiegler–Kedem models. The two other groups describe the transport of solutes as a function of structural and physicochemical parameters, and take into account membrane properties. These models are the solution diffusion and pore-flow models, respectively. Robinson et al. [12] studied the permeation of low-polarity solutes in a mixture of xylene isomers and found that the degree of cross-linking affects the permeance and selectivity of PDMS membranes by changing the swelling degree. The Spiegler–Kedem model could be applied across the entire range of membranes studied, whereas the applicability of the solution–diffusion model was diminished when the degree of swelling was large, suggesting that a potential transition between solution–diffusion and pore-flow mechanisms could occur as a function of the swelling degree. Han et al. [13] and White [14] concluded that solution diffusion type models describe the transport of mixtures of alkanes and aromatic compounds in toluene through PI (P84) membranes better than pore-flow models. Leitner et al. [15] reported that the Hagen–Poiseuille pore-flow model better explained some of the tendencies of the solvent permeance through swollen PDMS membranes, which usually described in terms of solution–diffusion mechanism [16]. It is still challenging to establish which model provides the best description for some types of organic solvent nanofiltration membranes. Furthermore, the generalization of the modelling strategy is complicated by the fact that the same membrane can behave differently in different solvents, when swelling comes into play.

In an effort to understand the transport mechanisms of dye compounds in alcoholic solvents through organic solvent nanofiltration membranes, herein, filtration experiments were carried out for ten dye solutes in methanol or ethanol solvents with two types of polymeric nanofiltration membranes. And a simplified permeation model has been modified on the base of Donnan-steric-pore model (DSPM) to explore the transport.

2. Experimental

2.1. Materials and methods

The polymeric membranes used were Desal-DK and Desal-DL nanofiltration membranes (Osmonics, Vista, CA, USA). They were negatively charged flat sheet composite multi-layered membranes, of which the top layer was polyamide material. Membrane properties are summarized in Table 1 [7].

Ten solutes that were selected based on their molecular weight, charge and detectability. Table 2 lists the physical properties of solutes used. Concentrations of the solutes were determined by UV-VIS-spectrophotometer (UV759, China) except for polyethylene glycol (PEG). For analysis of PEG, total organic carbon (TOC) analyzer (GE Innov0x, USA) was used. Methanol and ethanol (A.R. grade) were selected as solvent and their physical properties are shown in Table 3. All components were supplied by Sinopharm Chemical Reagent Co., Ltd., (China) and had initial purities in excess of 99%.

2.2. Research procedure

First of all, filtration experiments were carried out for ten dye solutes in methanol or ethanol solvents with two types of polymeric nanofiltration membranes to obtain flux and rejection data. Next, rejection and operating pressure data of three neutral solutes were fitted by the modified transport model to obtain an average pore radius parameter

Table 1
Membrane characteristics as indicated by manufacturer

Type	Manufacture	Property/Charge	Material	Molecular weight cut-off	Surface tension	Rejection
Desal-DK	Osmonics	Hydrophilic/Negative	Polyamide	180–300	58.0	98%[a]
Desal-DL	Osmonics	Hydrophilic/Negative	Polyamide	180–300	59.7	98%[a]

[a]2‰ $MgSO_4$ in water.

Table 2
Physical properties of the solutes

Solute	Code name	Formula	Charge	Molecular weight	Detection wavelength (nm)
Acid blue	A	$C_{20}H_{14}N_2O_5SNa$	Negative	416	558
Orange II	B	$C_{16}H_{12}N_2O_4SNa$	Negative	350	482
Acid fuchsin	C	$C_{20}H_{19}N_3O_9S_{32}Na$	Negative	587	552
Safranine O	D	$C_{20}H_{19}ClN_4$	Positive	351	534
Methylene blue	E	$C_{16}H_{18}ClN_3O_3S$	Positive	374	656
Crystal violet	F	$C_{25}H_{30}ClN_3$	Positive	408	580
PEG400	G	/	Neutral	400	/
PEG600	H	/	Neutral	600	/
Bromothymol blue	I	$C_{27}H_{28}Br_2O_5S$	Neutral	624	422
PEG200	J	/	Neutral	200	/

of the membrane. Last, rejection data of the other neutral solute and charged solutes were predicted with the obtained average pore radius, the predicted data were then compared with experimental data to examine the suitability of the modified model and discuss the probable transport mechanisms.

2.3. Performance of polymeric nanofiltration

Filtration experiments were carried out on a laboratory-scaled cross-flow membrane set-up as described in Fig. 1. The solute-solvent mixture was added to the reservoir from which an air-driven pump delivered the fluid to the membrane module via a variable area flow meter and a flow control valve. The permeate stream could either be circulated back to the reservoir or collected separately for subsequent sample analysis. The retentate stream returned to the reservoir which a cooler was employed to maintain the temperature of the circulating fluid. Transmembrane pressure and crossflow rate were controlled by the back-pressure regulator and the flow control valve. The circular, flat sheet membrane was mounted in a standard, and unmodified, Osmonics DESAL membrane module which gave a wetted surface area of 81 cm^2. Feed concentration of 0.1 mM was prepared in pure methanol or ethanol. A transmembrane pressure from 0.7 to 2.1 MPa was applied. The feed flow was set constant at 4 L/min, corresponding to a cross-flow velocity of 1.3 m/s. Calculated Reynolds number was 15 × 10^3 and turbulence was therefore guaranteed. Temperature was maintained at 25°C ± 1°C. Since low solution concentration was adopted, osmotic pressure, concentration polarization and membrane fouling could be neglected. Solvent flux (J_v) was determined by Eq. (1):

$$J_v = \frac{V}{A \times t} \tag{1}$$

where V (L) is the total volume of solvent permeated through tested membrane with a filtration area of A (m^2) during filtration time t (h). The solute rejection was determined by Eq. (2):

$$R = \frac{C_f \times C_p}{C_f} \times 100 \tag{2}$$

where C_f and C_p were the solute contents of feed and permeate streams, respectively.

2.4. Model modification

As neutral solute in aqueous media transports through nanofiltration membranes are dominated by convection and diffusion according to the Donnan-steric-pore model (DSPM) [17], molar flux of the solute (i), j_i is given by the extended Nernst–Planck Eq. (3):

$$J_i = -D_{i,p}\frac{dc_i}{dx} + K_{i,c}c_i J_v \tag{3}$$

where $D_{i,p}$ is pore diffusion coefficient of solute, c is concentration of solute, x is axial coordinate in membrane and $K_{i,c}$ is a hindrance factor accounting for the effects of pore walls on the motion of solute, which is given by Eq. (4):

$$K_{i,c} = \left(2 - \Phi_i\right)\left(1.0 + 00.054\lambda_i - 00.988\lambda_i^2 + 0.441\lambda_i^3\right) \tag{4}$$

where φ_i is dimensionless steric partition coefficient of solute and is defined by Eq. (5):

$$\Phi_i = \left(1 - \lambda_i\right)^2 \tag{5}$$

where λ_i is the dimensionless ratio of solute radius (r_i) to effective membrane pore radius (r_p) given as follows:

$$\lambda_i = \frac{r_i}{r_p} \tag{6}$$

The pore diffusion coefficient is given by Eq. (7):

$$D_{i,p} = K_{i,d}D_{i,\infty}\frac{\eta_0}{\eta} \tag{7}$$

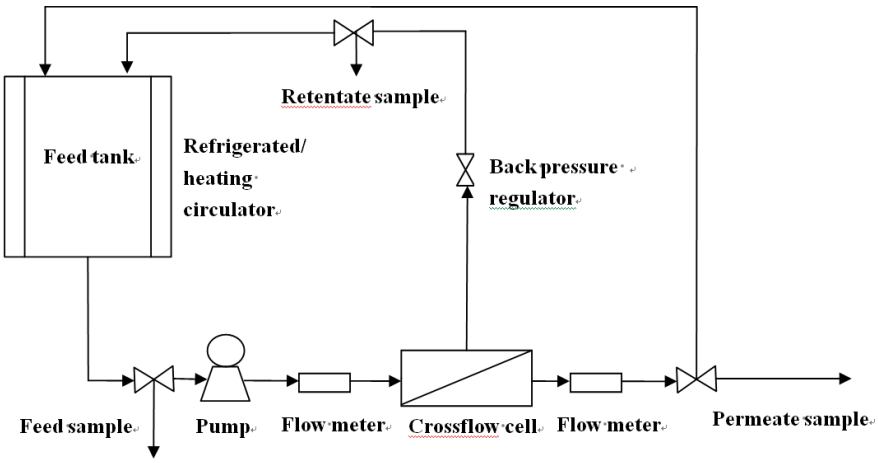

Fig. 1. Nanofiltration apparatus flowchart.

where $K_{i,d}$ is the hindrance factor for diffusion accounting for the effects of membrane pores to reduce solute–solvent diffusion coefficient below its value in the free bulk solution, and is given by Eq. (8):

$$K_{i,d} = 1.0 - 2.30\lambda_i + 1.154\lambda_i^2 + 0.224\lambda_i^3 \tag{8}$$

As per Eq. (7), the pore diffusion coefficient of solute is affected by the change in viscosity (η) inside the pore and bulk solvent. Viscosity inside the pore increases by a decrease in the pore radius such that viscosity ratio is given by:

$$\frac{\eta}{\eta_0} = 1.0 + 18\left(\frac{d}{r_p}\right) - 9\left(\frac{d}{r_p}\right)^2 \tag{9}$$

where η is bulk solvent viscosity, η_0 is viscosity inside the pore, d is the thickness of the oriented solvent layer.

$D_{i,\infty}$ is diffusive coefficient of solute in water at infinite dilution. The diffusive coefficient of solute in solvent can be expressed by the Wilke–Chang equation [18]:

$$D_{i,\infty} = 7.4\times10^{-8}\left(\alpha M\right)^{1/2}\frac{T}{\eta V_i^{0.6}} \tag{10}$$

where T is the absolute temperature, V_i is molar volume of solute at boiling point, α is association coefficient, 2.6, 1.9 and 1.5 for water, methanol and ethanol, respectively [18]. M is molecule weigh of solvent.

In non-aqueous nanofiltration, the influence of solvent on the size of solute must be taking into account. According to the Stokes–Einstein equation [19], the relationship between radius of solute and diffusive coefficient follows:

$$D_{i,\infty} = \frac{RT}{6\pi\eta r_i N_A} \tag{11}$$

where N_A is Avogadro constant, R is universal gas constant. Eq. (12) can be obtained by combining Eqs. (10) and (11) as follows:

$$\frac{r_{i1}}{r_{i2}} = \left(\frac{\alpha_2 M_2}{\alpha_1 M_1}\right)^{1/2} \tag{12}$$

In which 1 and 2 represent water and solvent, respectively. The radius of solute in solvent can be thus obtained with the known radius in water. Table 4 lists the effective radius of neutral solutes in methanol and ethanol calculated through Eq. (12).

For uncharged solutes, solute rejection is given by Eq. (13) according to the Donnan-steric-pore model [17]:

$$R = 1 - \frac{\left(K_{i,c} - \beta_i\right)\Phi_i}{1 - \left[1 - \left(K_{i,c} - \beta_i\right)\Phi_i\right]\exp\left(-P_{ei}\right)} \tag{13}$$

where β_i is a dimensionless quantity and P_{ei} is dimensionless modified Peclet number given by the equations:

$$\beta_i = \frac{8\eta}{RTr_p^2} D_{i,p} V_i \tag{14}$$

$$P_{ei} = \frac{\left(K_{i,c} - \beta_i\right) r_p^2 \Delta P}{8\eta D_{i,p}} \tag{15}$$

Eqs. (13)–(15) show that rejection of uncharged solute is independent of thickness of the membrane. The effective pore radius (r_p) of the membrane can be obtained by fitting experimental data (rejection (R) and operating pressure (ΔP)) through Eq. (13) with the known solute radius (r_i). Analogously, the rejection of the uncharged solute can be predicted with a given operating pressure, effective pore radius and solute radius.

3. Results and discussion

3.1. Influence of solvent, membrane and solute on solvent flux

The influence of solvent on solvent flux is shown in Fig. 2. As can be seen, at the operating pressure of 1.1 MPa, the average methanol flux was 97 L/h·m² for Desal-DK membrane and 119 L/h·m² for Desal-DL membrane; the average ethanol flux was 32 and 35 L/h·m² for Desal-DK and Desal-DL membrane respectively. With the same operation conditions, regardless of the solutes, the methanol flux was higher than the ethanol flux for both Desal-DK and Desal-DL membranes. From these results, it is concluded that the solvent has significant influence on membrane flux. According to Geens et al. [7], solvent flux is dependent on solvent viscosity, molecular size and difference in surface tension between membrane and solvent, and can be expressed as:

$$J_v \cdot \frac{V_m}{\eta \cdot \Delta\gamma} \tag{16}$$

where V_m is solvent molar volume and Δγ is the difference in surface tension between membrane and solvent. Since

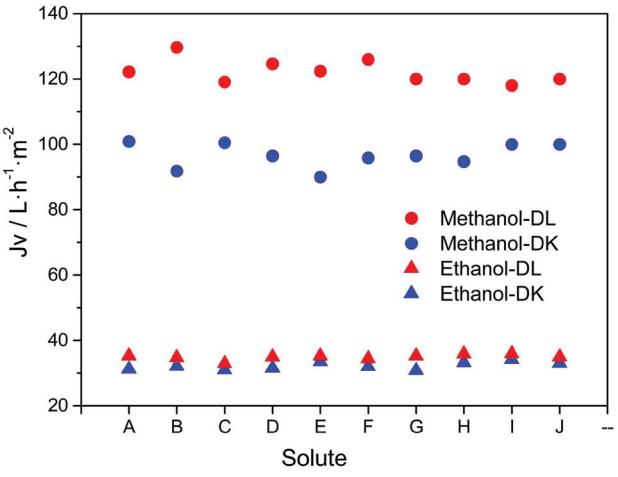

Fig. 2. Solvent flux of Desal-DK and Desal-DL membranes with different solutes.

Table 3
Physical properties of the solvents

Solvent	MW (g/mol)	Viscidity 10^{-3} (Pa·s)	Surface tension (mN/m)	Dielectric constant	Molar volume (cm^3/mol)
Methanol	32	0.61	22.55	31.2	40.4
Ethanol	46	1.17	22.27	25.7	58.4

methanol has lower viscosity, molar volume than ethanol, and has almost the same surface tension (Table 3), while the difference of viscosity dominate flux than the difference of molar volume, therefore the flux of methanol is higher.

The influence of membrane on solvent flux is also shown in Fig. 2. As can be seen, although those two membranes had the same molecular weight cut-off (Table 1), solvent fluxes of the Desal-DL membrane were always higher than that of the Desal-DK membrane for a certain solvent, regardless of the solutes. Solvent flux is not only depends on properties of solvent as mentioned above, but also dependents on properties of membrane. As Desal-DK and Desal-DL membrane top layer were made of polyamide, they have almost the same hydrophobicity and surface tension (58.0 and 59.7 mN/m for DK and DL membrane, respectively, Table 1). But according to Geens et al. [9], the average pore radius of Desal-DL membrane is somewhat larger than Desal-DK membrane (0.55–0.72 nm for Desal-DL and 0.52–0.64 nm for Desal-DK in methanol), so the solvent flux of Desal-DL membrane would be larger than Desal-DK membrane at the same filtration condition with the same solvent. It is concluded that solvent flux of the membrane in non-aqueous nanofiltration is also dominated by membrane structure parameters such as the pore size.

The influence of solute molecular weight and charge on solvent flux can be seen from Fig. 2. No significant differences in solvent fluxes were observed for each solvent-membrane combination. Since diluted feed solution (0.1 mM) was used, solute molecular weight and charge may have no significant impact on solvent flux. The small variation in solvent fluxes was due to measurement deviation (different membrane samples). Although the solute charge has no effect on solvent flux, it may have an effect on its rejection as discussed in next section.

3.2. Influence of solvent, membrane and solute on solute rejection

The influence of solvent on the solute rejection is shown in Fig. 3a and b. As can be seen, at the operating pressure of 1.1 MPa, the solute rejection in methanol was always higher than in ethanol for a certain solute and membrane. Since solute transport appears to be dominated by viscous flow [20], it can be assumed that solute rejection in non-aqueous nanofiltration is strongly influenced by steric hindrance. The variety of rejections in methanol and ethanol can be attributed to solute "salvation effects", which was confirmed by Geens et al. [21] that solvent–solute interactions (salvation) cause a different effective solute diameter in each solvent: it is smaller in ethanol than in methanol (Table 4), resulting in lower rejections in ethanol than in methanol.

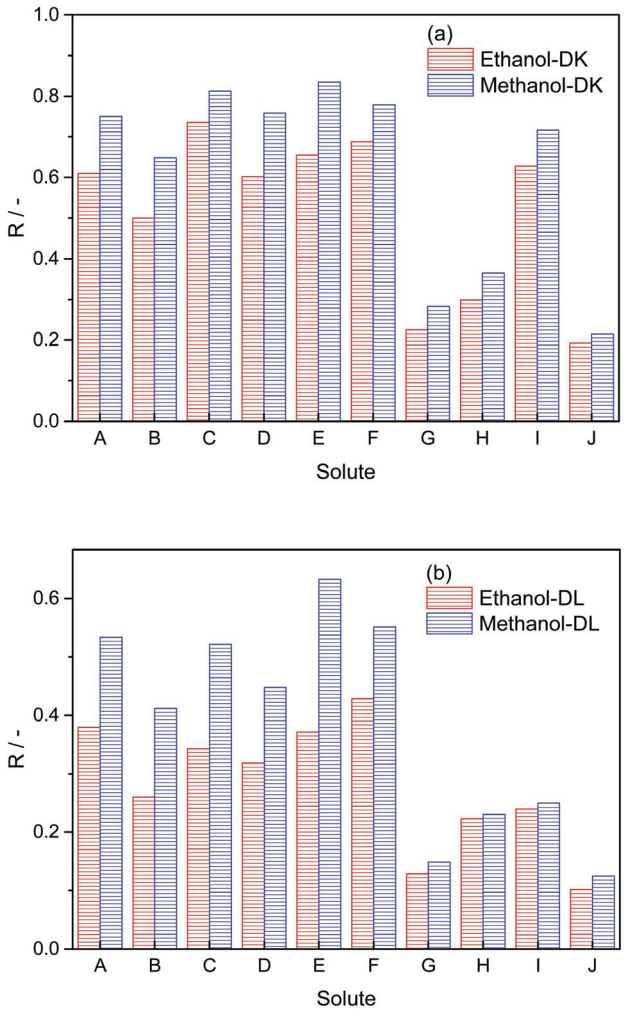

Fig. 3. Rejection of solute at 1.1 MPa. (a) Desal-DK membrane and (b) Desal-DL membrane.

The influence of membrane properties on the solute rejection is also shown in Fig. 3a and b. As can be seen, for a specific solution, the solute rejections of the Desal-DK membrane were higher than those of the Desal-DL membrane. As solute transport through nanofiltration membranes is mainly dominated by steric hindrance, solute molecule would experiences more difficulties in transporting the Desal-DK membrane pores than in Desal-DL membrane pores which has larger average pore radius as mentioned before.

The influence of solute molecular weight on the rejection is also can be seen from Fig. 3a and b. It seems no significant correlation between the rejection and the molecular weight could be obtained at the first sight. It's

true for the negatively or positively charged solutes. But the rejections of neutral solutes increased with molecular weights. For example, rejections of PEG200, PEG400 and PEG600 in ethanol were 19.3%, 22.6% and 29.9% for the Desal-DK membrane, respectively.

In the first instance, it might be unusual to consider the role of charges in organic solvents. According to the Debye–Huckel theory [22], however, the thickness of a double layer around an ion is proportional to the square root of the dielectric constant of the surrounding medium. It means that a charge exerts its influence over a longer distance in solvent with high dielectric constant. With the dielectric constant of methanol and ethanol being 31.2 and 25.7 at 298 K, respectively [23], the influence of a charge will indeed be smaller in alcohols, but still existing. In this way, charge effect might be introduced as an additional influence on rejection as common exists in aqueous nanofiltration. These are indeed the solutes that can dissociate (whatever negatively or positively charged) had higher rejections than neutral solutes with approximate molecular weight as shown in Fig. 3a and b, such as negative Crystal violet and positive Acid blue vs. neutral PEG400. The positively charged solutes also had higher rejections than negatively charged solutes with approximate molecular weight, such as Safranine O vs. Orange II, and Acid blue vs. Crystal violet. This may be attributed to solute-membrane interactions, as for the negatively charged solutes, a excluded force from the negatively charged Desal-DK membrane exists besides steric effect; as for positively charged solutes, they could be absorbed on the membrane surface and thus the rejections were enhanced; but for neutral solutes, there was only steric effect between the membrane and the solute, resulting the lowest rejections.

Table 4
Effective radius of neutral solutes in methanol and ethanol

Solute	Code name	Effective radius (nm)	
		Methanol	Ethanol
PEG400	G	0.393	0.369
PEG600	H	0.469	0.441
Bromothymol blue	I	0.481	0.452
PEG200	J	0.290	0.272

3.3. Modeling

In the modeling of the neutral solute transports through the membrane in non-aqueous nanofiltration, the first step is parameter fitting by Eq. (13), through which the effective pore radius of the membrane can be obtained. Table 5 shows the modeling parameters for PEG200 performed in methanol with Desal-DK membrane at 1.38 MPa as an example.

Fig. 4 shows the fitting curves of the neutral solute rejections with operating pressures. As can be seen, the experimental data were well fitted by the modified DSPM model. The fitting results are listed in Table 6. As shown, fitted effective membrane pore radius was influenced by the modeling solute. When the effective radius of modeling solute gets larger, the fitted effective membrane pore radius gets larger. It is consistent with reports that modeled in aqueous nanofiltration [19,24,25]. Table 6 also shows that the effective membrane pore sizes in ethanol are larger than in methanol for each of the membrane. As a result, besides the "salvation effects" of solutes, the membrane pore size was also a factor that made the solute rejections in methanol higher than in ethanol. The fitting results also showed that the membrane pore size of the Desal-DL membrane was larger than the Desal-DK membrane in each solvent, which has been discussed before.

In order to examine the feasibility of the modified model, the rejections of neutral solute Bromothymol blue (I) were predicted and compared with experimental data. Table 5 shows the predicting parameters for Bromothymol blue performed in methanol with Desal-DK membrane at 1.38 MPa as an example. Simultaneously, rejections of the negatively charged solute Orange II (B) and the negatively charged solute Methylene blue (E) were also predicted for the sake of investigating the influence of solute charge on modeling. Fig. 5 shows the modeling results of the Desal-DK membrane performed in methanol. As can be

Table 5
Modeling parameters for PEG200 and predicting parameters for Bromothymol blue performed in methanol with Desal-DK membrane at 1.38 MPa

Modeling			Predicting		
Input parameter	Input value	Output parameter (r_p)	Input parameter	Input value	Output parameter (R)
T	298.15		T	298.15	
ΔP	1.38E6		ΔP	1.38E6	
R	0.2186		r_p	1.159	
η	0.921E-3		η	0.898E-3	
r_i	0.29	0.872	r_i	0.481	0.751
V_i	178		V_i	425.67	
α	1.9		α	1.9	
M	32.042		M	32.042	
$D_{i,\infty}$	0.8344E-8		$D_{i,\infty}$	0.5072E-8	

Table 6
Fitted effective membrane pore radius by the modified model

Solute	Effective membrane pore radius (nm)			
	Desal-DK		Desal-DL	
	Methanol	Ethanol	Methanol	Ethanol
PEG200	0.872 ± 0.004	1.058 ± 0.025	1.409 ± 0.026	1.5672 ± 0.012
PEG400	1.227 ± 0.005	1.322 ± 0.024	1.611 ± 0.010	1.772 ± 0.018
PEG600	1.378 ± 0.016	1.506 ± 0.007	1.767 ± 0.009	1.809 ± 0.010
Average value	1.159 ± 0.008	1.295 ± 0.019	1.596 ± 0.015	1.716 ± 0.013

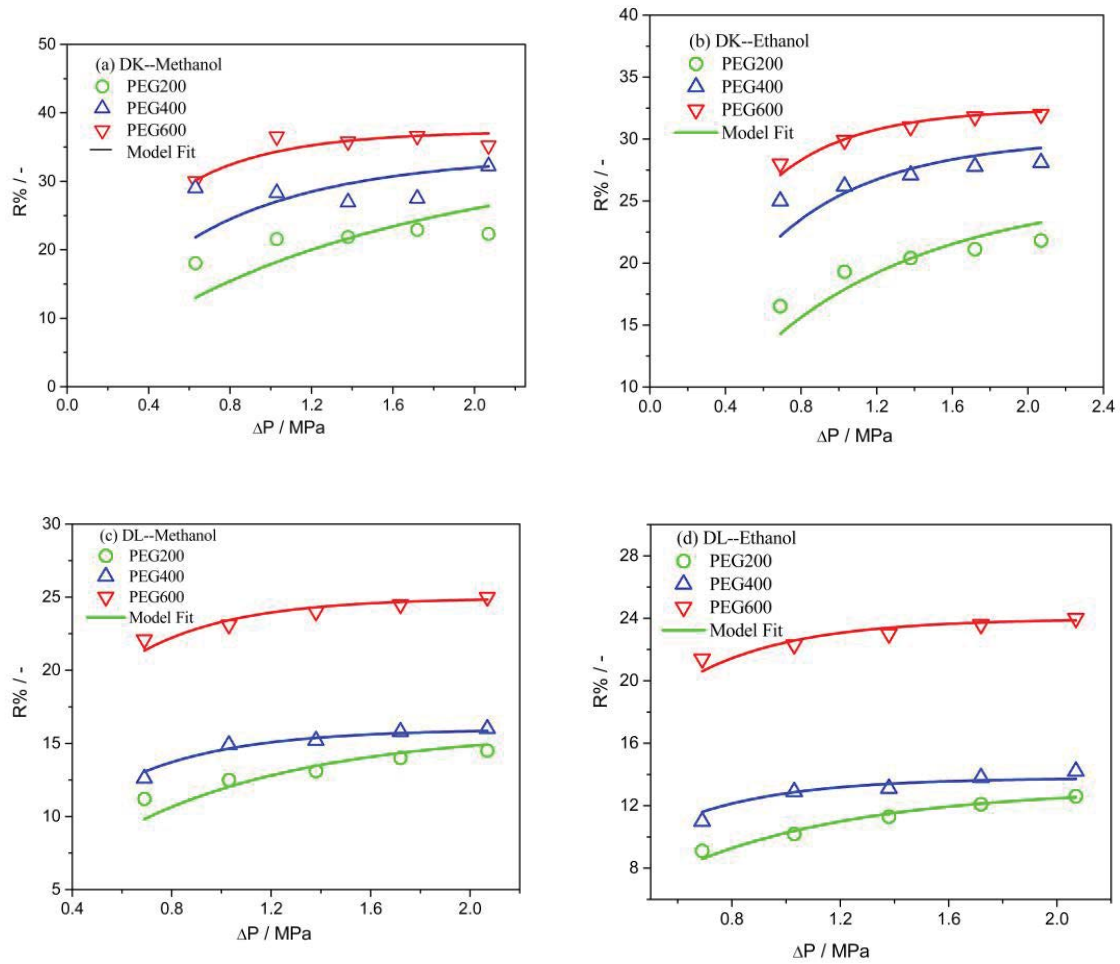

Fig. 4. Experimental data fitted by the modified DSPM model (a) DK-Methanol, (b) DK-Ethanol, (c) DL-Methanol, and (d) DL-Ethanol.

seen, the predicted rejections of solute I were very close to the experimental data, but the predicted values of solute B or E were smaller than the experimental values obviously. From this point, it can be concluded that the modified model is applicable in the modeling of neutral solutes transport through nanofiltration membranes in non-aqueous media, but is not fit for the charged solutes. The charge of solute plays an important role in non-aqueous nanofiltration. Hussain et al. [17] indicated that there are three main effects affect the transport and selectivity of NF membranes: charge repulsion, steric/hydrodynamic and dielectric effects. The first effect is caused by the charged nature of the membrane and solutes, while the second effect is caused by the relative size of solutes to the membrane pores; third effect is caused by the differences in dielectric constant between bulk and membrane pore. The mathematical transport

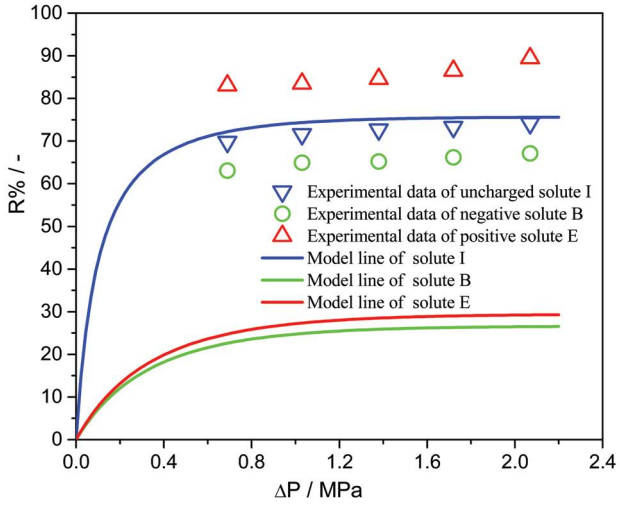

Fig. 5. Modeling line and experimental data of the Desal-DK membrane performed in methanol

model we modified currently only takes into account the second effect, which is why the model is not fit for charged solutes. Further modification of the model by adding charge density, dielectric constant and Donnan potential parameters that considering the affect of charge effect will be our next work. The other modeling results were similar to those shown in Fig. 5, which are not shown repeatedly here.

4. Conclusions

This work investigated the performance of polymeric membranes in non-aqueous nanofiltration. The effects of solvent, solute and membrane on the separation performance were discussed. And the Donnan-steric-pore nanofiltration transport model was modified for the non-aqueous nanofiltration. The main conclusions are as follows:

- The solvent fluxes of the Desal-DL membrane were always higher than that of the Desal-DK membrane for a certain solvent, regardless of the solutes. As for the specific nanofiltration membrane, methanol solution fluxes were always higher than that of ethanol solution. Solute molecular weight and charge had no influence on solvent flux at low solution concentration.
- For the specific solution, solute rejections of the Desal-DK membrane were higher than those of the Desal-DL membrane. For a certain solute and membrane, the rejection in methanol was always higher than that in ethanol. The rejections of neutral solutes increased with molecular weights. For the charged solutes, no significant correlation between rejection and molecular weight was obtained. For the solutes with approximate molecular weight, the order of rejection from highest to lowest was the positively charged solute, the negatively charged solute, and the neutral solute.
- The modified Donnan-steric-pore nanofiltration model (DSPM) was proved to be suitable to predict the rejection of neutral solute rather than charged solute in non-aqueous nanofiltration. The solvent had influences on the average pore radius of the membrane. Solute charge and solute–solvent-membrane interactions existed in non-aqueous nanofiltration systems.

Acknowledgements

The authors would like to acknowledge the financial support from National Natural Science Foundation of China (Nos. 21776115); Senior talents fund of Jiangsu University (12JDG088) and Jiangsu Planned Projects for Postdoctoral Research Funds (1301059B).

Symbols

A	—	Area, m^2
C	—	Concentration, mol/m^3
d	—	Thickness of the oriented solvent layer, 0.28 nm
$D_{i,p}$	—	Pore diffusion coefficient, cm^2/s
$D_{i,\infty}$	—	Solute bulk diffusion coefficient, cm^2/s
j_i	—	Molar flux of solute, $mol/(m^2 \cdot s)$
J_v	—	Solvent flux, $L/(m^2 \cdot h)$
$K_{i,c}$	—	Hindrance factor for convection, dimensionless
$K_{i,d}$	—	Hindrance factor for diffusion, dimensionless
M	—	Molecule weigh of solvent, g/mol
N_A	—	Avogadro constant, $6.02 \times 10^{23}/mol$
P_{ei}	—	Modified Peclet number, dimensionless
ΔP	—	Operating pressure, N/m^2
r_i	—	Radius of solute, m
r_p	—	Effective pore radius, m
R	—	Rejection, %
t	—	Time, h
T	—	Absolute temperature, K
V_i	—	Molar volume of solute at boiling point, cm^3/mol
x	—	Axial position within the pore, m

Greek

α	—	Association coefficient, dimensionless
β	—	Ion function, dimensionless
γ	—	Surface tension, N/m
η	—	Bulk solvent viscosity, $N \cdot s/m^2$
η_0	—	Solvent viscosity within pores, $N \cdot s/m^2$
λ	—	Ratio of solute radius to membrane pore radius, dimensionless
ϕ	—	Steric partition coefficient, dimensionless

Subscripts

1	—	Water
2	—	Solvent
f	—	Feed
i	—	Solute
p	—	Permeate

References

[1] C. Cheng, S.A. Iyengar, R. Karnik, Molecular size-dependent subcontinuum solvent permeation and ultrafast nanofiltration across nanoporous graphene membranes, Nat. Nanotechnol., 16 (2021) 989–995.
[2] K. Rezzadori, F.M. Penha, M.C. Proner, G. Zin, J.C.C. Petrus, M.D. Luccio, Impact of organic solvents on physicochemical

properties of nanofiltration and reverse-osmosis membranes, Chem. Eng. Technol., 42 (2019) 2700–2708.
[3] J.J. Torres, J.T. Arana, N.A. Ochoa, J. Marchese, C. Pagliero, Biodiesel purification using polymeric nanofiltration composite membranes highly resistant to harsh conditions, Chem. Eng. Technol., Special Issue: Membrane Separation, 41 (2018) 253–260.
[4] R. Zhang, J. Xue, Y. Li, B. Cao, P. Li, A chemical imidization method to avoid pore collapsing and selective layer thickening of PMDA-ODA polyimide nanofiltration membranes, Desal. Water Treat., 115 (2018) 33–44.
[5] P. Marchetti, A.G. Livingston, Predictive membrane transport models for organic solvent nanofiltration: how complex do we need to be?, J. Membr. Sci., 476 (2015) 530–553.
[6] Q.S. Xu, J.W. Jiang, Molecular simulations of liquid separations in polymer membranes, Curr. Opin. Chem. Eng., 28 (2020) 66–74.
[7] J. Geens, B. Van der Bruggen, C. Vandecasteele, Transport model for solvent permeation through nanofiltration membranes, Sep. Purif. Technol., 48 (2006) 255–263.
[8] L. Hesse, J. Micovic, P. Schmidt, A. Gorak, G. Sadowski, Modelling of organic-solvent flux through a polyimide membrane, J. Membr. Sci., 428 (2013) 554–561.
[9] J. Geens, K. Boussu, C. Vandecasteele, B. Van der Bruggen, Modelling of solute transport in non-aqueous nanofiltration, J. Membr. Sci., 281 (2006) 139–148.
[10] Y.H. Lu, Z.P. Qin, N.X. Wang, H.X. Guo, Q.F. An, Y.C. Liang, TiO_2-incorporated polyelectrolyte composite membrane with transformable hydrophilicity/hydrophobicity for nanofiltration separation, Chin. J. Chem. Eng., 28 (2020) 2533–2541.
[11] A.A. Yushkin, M.N. Efimov, A.O. Malakhov, G.P. Karpacheva, G. Bondarenko, L. Marbelia, I.F.J. Vankelecom, A.V. Volkov, Creation of highly stable porous polyacrylonitrile membranes using infrared heating, React. Funct. Polym., 158 (2021) 104793, doi: 10.1016/j.reactfunctpolym.2020.104793.
[12] J.P. Robinson, E.S. Tarleton, K. Ebert, C.R. Millington, A. Nijmeijer, Influence of cross-linking and process parameters on the separation performance of poly(dimethylsiloxane) nanofiltration membranes, Ind. Eng. Chem. Res., 44 (2005) 3238–3248.
[13] S.J. Han, S.S. Luthra, L. Peeva, X.J. Yang, A.G. Livingston, Insights into the transport of toluene and phenol through organic solvent nanofiltration membranes, Sep. Sci. Technol., 38 (2003) 1899–1923.
[14] L.S. White, Transport properties of a polyimide solvent resistant nanofiltration membrane, J. Membr. Sci., 205 (2002) 191–202.
[15] L. Leitner, C. Harscoat-Schiavo, C. Vallieres, Experimental contribution to the understanding of transport through polydimethylsiloxane nanofiltration membranes: influence of swelling, compaction and solvent on permeation properties, Polym. Test., 33 (2014) 88–96.
[16] H. Ben Soltane, D. Roizard, E. Favre, Effect of pressure on the swelling and fluxes of dense PDMS membranes in nanofiltration: an experimental study, J. Membr. Sci., 435 (2013) 110–119.
[17] A.A. Hussain, S.K. Nataraj, M.E.E. Abashar, I.S. Al-Mutaz, T.M. Aminabhavi, Prediction of physical properties of nanofiltration membranes using experiment and theoretical models, J. Membr. Sci., 310 (2008) 321–336.
[18] K. Miyabe, R. Isogai, Estimation of molecular diffusivity in liquid phase systems by the Wilke–Chang equation, J. Chromatogr. A, 1218 (2011) 6639–6645.
[19] D. Coglitore, S.P. Edwardson, P. Macko, E.A. Patterson, M. Whelan, Transition from fractional to classical Stokes–Einstein behaviour in simple fluids, R. Soc. Open Sci., 4 (2017) 170507, doi: 10.1098/rsos.170507.
[20] B. Van der Bruggen, J. Geens, C. Vandecasteele, Fluxes and rejections for nanofiltration with solvent stable polymeric membranes in water, ethanol and n-hexane, Chem. Eng. Sci., 57 (2002) 2511–2518.
[21] J. Geens, A. Hillen, B. Bettens, B. Van der Bruggen, C. Vandecasteele, Solute transport in non-aqueous nanofiltration: effect of membrane material, J. Chem. Technol. Biotechnol., 80 (2005) 1371–1377.
[22] P.W. Atkins, J.D. Paula, Physical Chemistry, 8th ed., Oxford University Press, Oxford, UK, 2006.
[23] R.C. Weast, M.J. Astle, CRC Handbook of Chemistry and Physics, 70th ed., CRC Press, Boca Raton, Florida, USA, 1989.
[24] J. Schaep, C. Vandecasteele, A.W. Mohammad, Modelling the retention of ionic components for different nanofiltration membranes, Sep. Purif. Technol., 22–23 (2001) 169–179.
[25] W.R. Bowen, B. Cassey, P. Jones, Modelling the performance of membrane nanofiltration-application to an industrially relevant separation, J. Membr. Sci., 242 (2004) 211–220.